XPS CHARACTERIZATION OF Mo-Nb MIXED-OXIDE NANOROD ARRAYS VIA THE ANODIZING OF THIN Al/Mo-Nb-ALLOY BILAYERS ON SUBSTRATES

[1]Maria BENDOVA, [1,2]Jan PRASEK, [1]Alexander MOZALEV

[1]Department of Microelectronics, Faculty of Electrical Engineering and Communication, Brno University of Technology, Brno, Czech Republic, EU, bendova@vutbr.cz, mozalev@vutbr.cz

[2]CEITEC – Central European Institute of Technology, Brno University of Technology, Brno, Czech Republic, EU, prasek@vutbr.cz

https://doi.org/10.37904/nanocon.2025.4993

Abstract

Molybdenum oxides form a large group of materials resulting from the ability of Mo to possess different formal oxidation states and local coordinations, which may give rise to mixed-valency oxides indispensable for energy storage, gas sensing, electrochromic or catalytic applications. Nanostructuring and doping molybdenum oxides with foreign elements or mixing with similar or dissimilar metal oxides may substantially advance the properties of the individual oxide, although such an approach typically requires exceptionally high temperatures, high vacuum, and high-budget equipment. In this work, we present an alternative approach to creating arrays of molybdenum oxide mixed with niobium oxide nanostructures via a simple, self-organized, room-temperature electrochemical anodizing of thin Al layers superimposed on thin Mo-Nb metal-alloy layers of variable component concentrations prepared by the magnetron sputter-deposition. Anodizing was carried out in oxalic acid solution, forming porous anodic alumina (PAA), followed by PAA-assisted oxidation of the alloy underlayers, and finishing with selective dissolution of the PAA overlayers. Detailed X-ray photoelectron spectroscopy (XPS) analysis of Mo 3d and Nb 3d narrow-scan spectra revealed that the highest amount of Mo in the nanostructures' surface was 79 at.% (Mo+Nb=100 at.%). The dominating molybdenum-oxide component comprised Mo cations with various oxidation states (Mo^{6+}, Mo^{5+}, Mo^{4+}, and Mo^{3+}), whereas the niobium-oxide inclusions were mostly Nb_2O_5. The success of preparing and analyzing the Mo-Nb mixed-oxide nanostructures is vital for understanding the formation-structure-morphology relationship and exploring the functional properties of the novel nanoarrays.

Keywords: Anodic oxidation, metal oxides, molybdenum, niobium, X-ray photoelectron spectroscopy

1. INTRODUCTION

Molybdenum oxides (MoO_x) reveal diverse electronic properties attributed to various formal oxidation states and local coordination of Mo cations, giving rise to mixed-valency oxides [1]. Molybdenum oxides have been applied for constructing energy storage and conversion, electrochromic, gas sensing, and photo- and electrocatalytic devices [2]. For metal oxides in general and MoO_x specifically, nanostructuring to produce nanowires, nanorods, or nanotubes substantially improves the oxide functional properties [3]. This is due to an increased surface-to-volume ratio and/or shorter carrier transport pathways compared with bulk materials [4]. Moreover, doping or mixing molybdenum oxides with similar or dissimilar metal oxides may substantially advance the properties of the individual oxides, although associated techniques typically require exceptionally high temperatures, high-vacuum conditions, and high-budget equipment.

An alternative approach for creating MoO_x-based nanostructures self-organized on a substrate could be based on the PAA-assisted anodizing of valve metals, as was reported for Ta, Nb, W, Ti, Hf, Zr, or some alloys [5]. This results in the formation of short oxide nanoprotrusions of the underlying metal in the PAA barrier layer.

Further re-anodizing to a higher voltage extends the oxide protrusions into the PAA nanopores, forming metal-oxide nanorods following the morphology of the PAA layer. A layer of molybdenum alloy must be used instead of pure molybdenum to obtain the mixed-oxide nanorods. The oxide mixing should be advantageous since there have been no reports on a successful PAA-assisted anodizing of pure molybdenum due to the peculiar electrochemical behavior of molybdenum and the instability of molybdenum oxides in aqueous electrolytes [1,6]. We have selected Nb as the alloying element because it behaves electrochemically as a typical valve metal, and its oxide has excellent chemical stability [5,7]. In this work, we have anodized an Al/Mo-Nb-alloy bilayer in an oxalic acid solution to prepare novel MoO_x-Nb_2O_5 nanostructure arrays. The chemical composition of nanoarrays, mainly the Mo and Al contents and the stoichiometry of the oxides, has been investigated by X-ray photoelectron spectroscopy (XPS).

2. EXPERIMENTAL PART

2.1 Sample preparation

The precursor thin-film Al/Mo-Nb-alloy bilayer was prepared on an oxidized Si wafer by the magnetron co-sputtering of a 200-nm thick Mo-Nb alloy layer followed by sputtering of a 700-nm thick Al layer using Mo (99.95%), Nb (99.95%), and Al (99.999%) targets. 1 cm × 1 cm samples were cut from the wafer and galvanostatically anodized at a steady-state voltage of 50 V in 0.6 M oxalic acid at room temperature. For selected samples, re-anodizing was performed in a borate buffer (0.5 M H_3BO_3/0.05 M $Na_2B_4O_7$) to a more anodic voltage of 180 V. The PAA overlayer was partially or fully selectively etched away in CrO_3/H_3PO_4-based etchant [5] to obtain the 'PAA-residues' or 'PAA-free' samples. Field-emission SEM, utilizing an InBeam detector for secondary electrons, was used to examine the morphology of the anodic films.

2.2 XPS investigation

XPS analysis was conducted in a Kratos Axis Ultra DLD spectrometer using a monochromatic Al Kα source. The X-ray emission power was 75 W with a 15 kV accelerating voltage focused to 300 μm × 700 μm. The emitted electrons were detected at fixed pass energies of 160 eV for the survey spectra and 20 eV for the high-resolution spectra. The Kratos charge neutralizer system was used for all specimens.

The spectra were analyzed using CasaXPS. GL(30) profiles were used for all components except the metallic core lines of Mo 3d and Nb 3d, for which asymmetric profiles in the form of LA(1.1,2,2) and LA(2,3.3,12) were applied, respectively. A standard Shirley background was used. Spectra from all samples were charge-corrected to give the adventitious C 1s spectral component (C−C, C−H) binding energy of 284.8 eV. The deconvolution of C 1s spectra was performed as described elsewhere [5,8].

3. RESULTS AND DISCUSSION

3.1 Film formation and morphology

The precursor Al/Mo-Nb-alloy bilayer was initially characterized by XPS to obtain the Nb content after selectively removing the Al overlayer in 1 wt.% NaOH solution. The presence of C, O, Mo, Nb, and Al was confirmed on the alloy surface. From the narrow scan Mo 3d and Nb 3d spectra, the Nb content was calculated to be 19 at.% (when Mo+Nb=100 at.%). Therefore, the alloy layer will be referred to as the Mo-19Nb and the initial bilayer as the Al/Mo-19Nb.

The PAA-assisted anodizing and re-anodizing of the Mo-19Nb layer, followed by selectively etching the PAA layer, resulted in an array of well-aligned oxide nanorods, as confirmed by SEM observations (**Figure 1**). The rods are about 400 nm long, anchored to the substrate via a compact bottom-oxide layer (**Figure 1a,b**). The lower parts of the rods (originally residing in the PAA barrier layer) are slightly narrower than their upper parts,

which are ~40 nm in diameter (**Figure 1c,d**). Therefore, the alloying of Mo with a small amount of Nb enabled stabilization of the growing oxide, preventing it from dissolving, which resulted in a successful PAA-assisted formation of MoO_x-based nanorods.

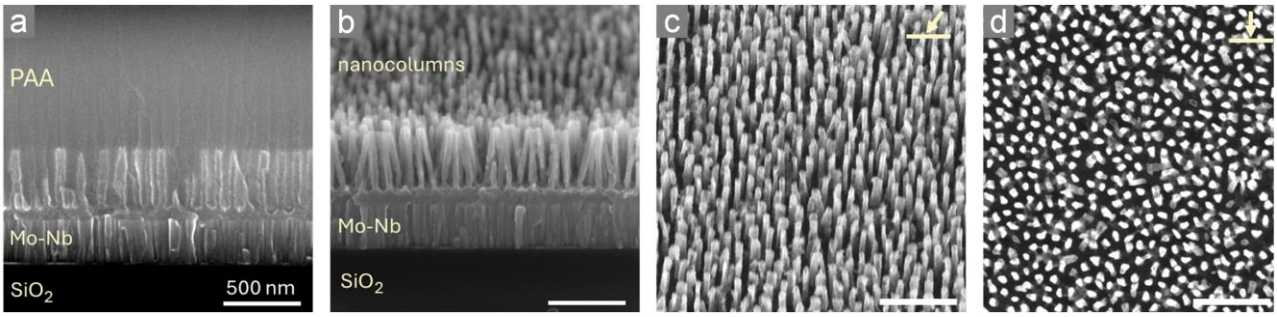

Figure 1 Cross-sectional, tilted, and top SEM views of (a) PAA-embedded and (b–d) PAA-free re-anodized anodic film prepared from the Al/Mo-19Nb bilayer

Based on the SEM observation, we have developed a schematic model describing the formation process for the anodized and re-anodized MoO_x-based nanofilms (**Figure 2**). The migration rates of Mo^{n+} and Nb^{n+} cations likely differ, and therefore, a compositional gradient along the nanorods is expected, as indicated by the colors in the schematics. For XPS analysis, we selected three films made from the Al/Mo-19Nb bilayer: the anodized PAA-free (**Figure 2e**), the re-anodized PAA-free (**Figure 2f**), and the re-anodized PAA-residues (**Figure 2g**) films. The third option was added to mask the bottom oxide layer and thus to distinguish XPS signals originating from various parts of the re-anodized film.

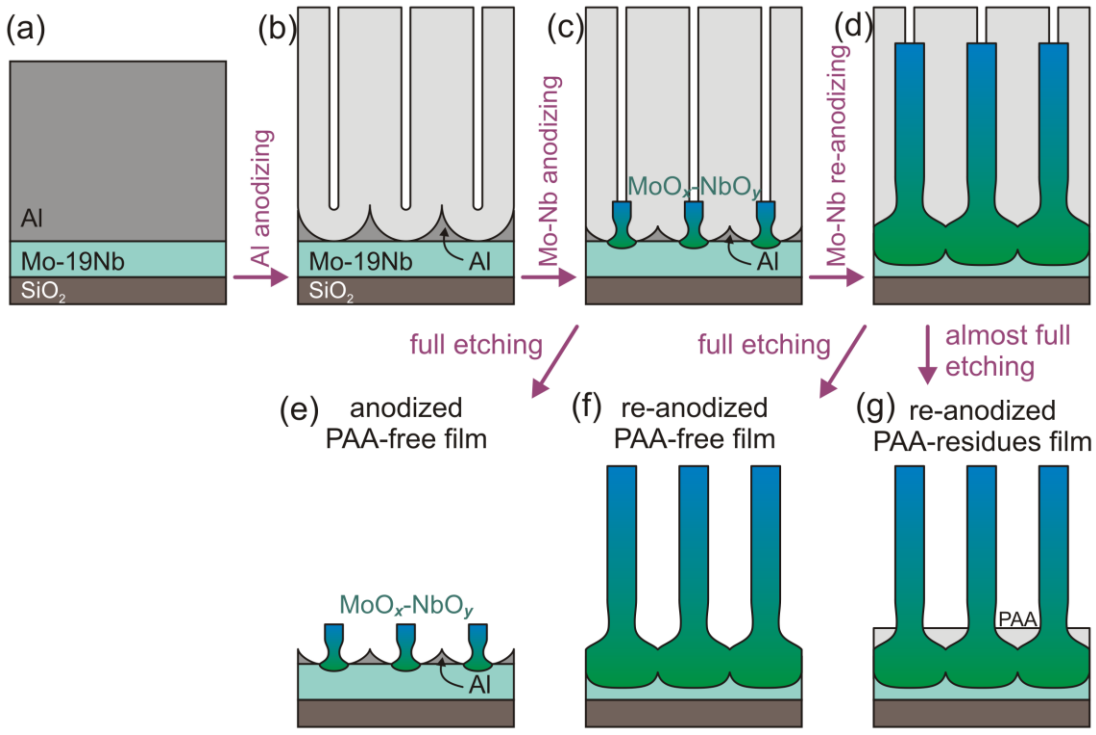

Figure 2 Schematic processes for forming MoO_x-based nanoarrays: (a) the sputter-deposition of an Al/Mo-19Nb bilayer onto an oxidized Si wafer, (b) the anodizing of the Al layer at 50 V to form a PAA film, (c) the anodizing of the Mo-19Nb alloy layer through the PAA barrier layer, and (d) the re-anodizing of the Mo-19Nb layer to 180 V; (e) the anodized PAA-free, (f) the re-anodized PAA-free, and (g) the re-anodized PAA-residues films

3.2 Chemical composition

XPS examination was performed on the anodized PAA-free, re-anodized PAA-free, and re-anodized PAA-residues films made from the Al/Mo-19Nb bilayer to estimate the film surface layers' chemical composition and bonding states. C, O, Mo, Nb, Al, P, and Cr were identified in the survey spectra; the last two elements were present due to the etching in the CrO_3/H_3PO_4-based solution. Narrow-scan C 1s, O 1s, Mo 3d, Nb 3d, and Al 2p spectra were collected to perform quantitative analysis and reveal the bonding states. The experimental and fitted Mo 3d, Nb 3d and Al 2p spectra are shown in **Figure 3**.

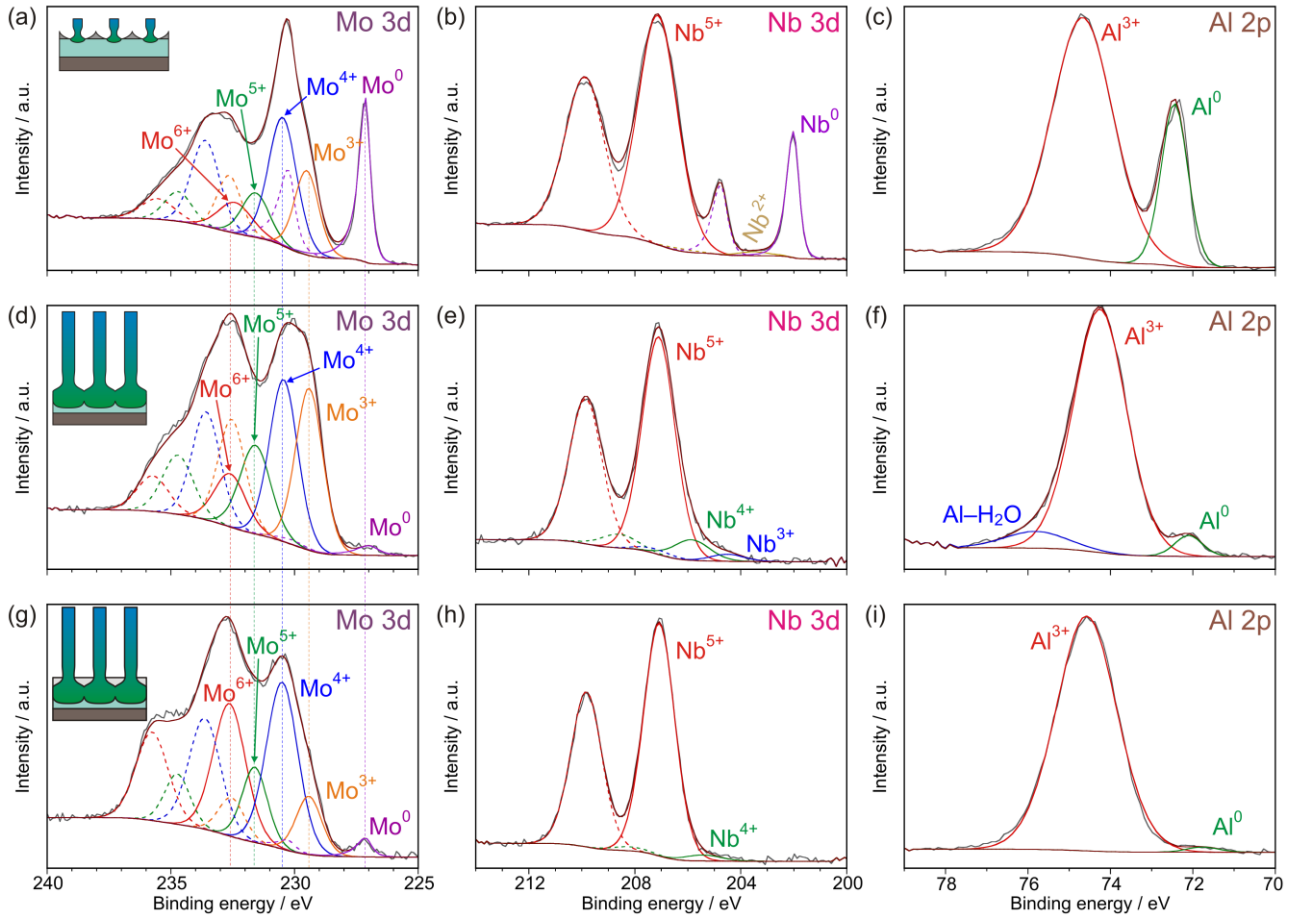

Figure 3 Experimental and fitted XPS spectra of the surface of the (a–c) anodized PAA-free, (d–f) re-anodized PAA-free, and (g–i) re-anodized PAA-residues anodic films

The *Mo 3d spectra* (**Figures 3a,d,g**) are fitted with several constrained doublets (Mo $3d_{5/2}$ and $3d_{3/2}$ with a fixed peak-separation energy of 3.13 eV and with a fixed intensity ratio of 3:2 [9,10]). All the films reveal the presence of four Mo^{n+} cations, with n = 6, 5, 4, or 3, in various ratios and a doublet of Mo^0. The Mo $3d_{5/2}$ positions agree with the literature values [9–11] and are consistent between the samples (as indicated by the vertical lines across the spectra), although the separation between the doublets is relatively small (~1.0 eV) and the assignment of the doublets to the specific oxidation states of Mo is, to some extent, questionable [9–11]. The high amount of Mo^0 in the anodized film (**Figure 3a**) is explained by the Mo-19Nb residues around the nanoprotrusions, whereas in the re-anodized films (**Figures 3d,g**), such metallic residues are not expected. When subtracting the Mo^0 contributions, an average calculated oxidation state of Mo in MoO_x in the anodic parts of the films is 4.2, 4.1, and 4.7 for the anodized PAA-free, re-anodized PAA-free, and re-anodized PAA-residues films, respectively. Clearly, the PAA-residues sample contains more oxidized MoO_x. This means the rod's surface contains more oxidized MoO_x compared with the bottom oxide.

The *Nb 3d spectra* (**Figures 3b,e,h**) are fitted with doublets of appropriately constrained peaks (Nb $3d_{5/2}$ and $3d_{3/2}$ with a fixed peak separation energy of 2.75 eV and with a fixed intensity ratio of 3:2 [5]). All the spectra contain a high-intensity doublet at the highest binding energy (with Nb $3d_{5/2}$ at 207.1±0.1 eV), assigned to Nb^{5+} cations in Nb_2O_5 [5]. The anodized sample (**Figure 3b**) reveals a substantial amount of Nb^0 [5] due to the metallic residues. Furthermore, minor amounts of suboxides Nb^{4+} (9%) and Nb^{3+} (3%) are identified in the re-anodized PAA-free film (**Figure 3e**). The PAA-residues sample has even fewer suboxides (**Figure 3h**). Therefore, similarly to MoO_x, the NbO_x in the nanorods is more oxidized than the bottom oxide layer.

After subtracting the metallic contributions, the fitted Mo 3d and Nb 3d narrow-scan spectra were also used to calculate the Mo content (when at.%(Mo+Nb)=100%) in the surface layer of the anodic parts of the films. Mo content decreases from 79 through 69 to 60 at.% for the anodized PAA-free, re-anodized PAA-free, and re-anodized PAA-residues films, respectively, whereas the initial Mo-19Nb alloy has 81 at.% Mo. This finding means that the surface layer of the anodic films contains both MoO_x and NbO_x in appreciable amounts; however, the amount of Mo is lower in the re-anodized samples than in the initial alloy, and it is substantially lower in the PAA-residues film. Thus, the rods contain less Mo than the bottom oxide, which implies that the Mo^{n+} cations migrate slower than the Nb^{n+} cations under the high electric field during the anodizing and re-anodizing processes.

The *Al 2p spectra* (**Figures 3c,f,i**) are fitted with a few singlet peaks. The highest-intensity peak is associated with Al_2O_3 [5]. In addition, a narrow Al^0 peak residing at 71.8–72.5 eV is noted in all the spectra. A relatively broader low-intensity peak in the spectrum of the re-anodized PAA-free sample, shifted to +1.6 eV from the Al_2O_3 position, is attributed to hydrated Al_2O_3 [12]. After subtracting the metallic contributions originating from the metallic residues surrounding the nanorods (and also the corresponding native oxide formed on the aluminum [13]), an approximate amount of Al in the surface layer of the anodic films is obtained (providing that at.%(Al+Nb+Mo)=100%): 68, 79, and 90 at.% Al for the anodized PAA-free, re-anodized PAA-free, and re-anodized PAA-residues films, respectively. An amount of Al up to 80% has been reported for PAA-assisted nanofilms made from various precursor metals. The higher amount of Al in the PAA-residues film is explained by underetched alumina between the lower parts of the oxide nanorods.

In summary, the surface layer of the anodic films contains MoO_x with an average oxidation state of Mo ~4.2, mixed with Nb_2O_5, substoichiometric niobium oxides, and Al_2O_3. The amount of Mo is lower than in the initial Mo-19Nb alloy. The surface of the oxide nanorods, compared with the whole surface of the re-anodized anodic film, has a relatively smaller amount of Mo, suggesting a slower migration of Mo^{n+} cations compared with Nb^{n+} cations, and comprises more oxidized Mo and Nb oxides, whereas the bottom oxide layer is composed of more reduced Mo and Nb oxides. The oxide nanorods' inner part is probably alumina-free mixed Mo-Nb anodic oxide [5].

4. CONCLUSIONS

In the present work, we report, for the first time, the electrochemical PAA-assisted synthesis of a MoO_x-based nanorod array made from the Al/Mo-19Nb-alloy bilayer. The alloying of Mo with a relatively low amount of Nb in the precursor material enabled the field-assisted growth of chemically stable mixed-oxide nanorods. The XPS analysis revealed that the rods' surface has a complex chemical composition comprising a dominating amount of MoO_3, Mo_2O_5, MoO_2, and Mo_2O_3 mixed with a minor amount of Nb_2O_5, NbO_2, and Nb_2O_3. Due to the interaction of growing Mo-Nb anodic oxide with the PAA cell walls, the rods' surface also contains Al_2O_3. A compositional difference between the various parts of the anodic film was suggested based on the XPS analysis.

Mixing molybdenum oxides with minor amounts of niobium oxides, likely at the nanoscale level, is expected to substantially impact the oxides' electrochemical, electronic, and electro-optical properties. With a focus on energy storage applications [6,7], the nanoarrays developed here will be the subject of future investigation.

ACKNOWLEDGEMENTS

The research leading to these results was supported by GACR grant no. 23-07848S. We acknowledge the use of CzechNanoLab Research Infrastructure supported by MEYS CR (LM2018110).

REFERENCES

[1] de CASTRO, I.A., DATTA, R.S., OU, J.Z., CASTELLANOS-GOMEZ, A., SRIRAM, S., DAENEKE, T., KALANTAR-ZADEH, K. Molybdenum oxides – From fundamentals to functionality. *Advanced Materials*. 2017, vol. 29, 1701619, pp. 31.

[2] CONCEPCIÓN, O., de MELO, O. The versatile family of molybdenum oxides: synthesis, properties, and recent applications. *Journal of Physics: Condensed Matter*. 2023, vol. 35, 143002, pp. 26.

[3] DEVAN, R.S., PATIL, R.A., LIN, J.-H., MA, Y.-R. One-dimensional metal-oxide nanostructures: recent developments in synthesis, characterization, and applications. *Advanced Functional Materials*. 2012, vol. 22, pp. 3326–3370.

[4] OSTERLOH, F.E. Inorganic nanostructures for photoelectrochemical and photocatalytic water splitting. *Chemical Society Reviews*. 2013, vol. 42, pp. 2294–2320.

[5] MOZALEV, A., VÁZQUEZ, R.M., BITTENCOURT, C., COSSEMENT, D., GISPERT-GUIRADO, F., LLOBET, E., HABAZAKI, H. Formation–structure–properties of niobium-oxide nanocolumn arrays via self-organized anodization of sputter-deposited aluminum-on-niobium layers. *Journal of Materials Chemistry C*. 2014, vol. 2, pp. 4847–4860.

[6] ELKHOLY, A.E., DUIGNAN, T.T., SUN, X., ZHAO, X.S. Stable *α*-MoO_3 electrode with a widened electrochemical potential window for aqueous electrochemical capacitors. *ACS Applied Energy Materials*. 2021, vol. 4, pp. 3210–3220.

[7] SHEN, F., SUN, Z., HE, Q., SUN, J., KANER, R.B., SHAO, Y. Niobium pentoxide based materials for high rate rechargeable electrochemical energy storage. *Materials Horizons*. 2021, vol. 8, pp. 1130–1152.

[8] PAYNE, B.P., BIESINGER, M.C., McINTYRE, N.S. X-ray photoelectron spectroscopy studies of reactions on chromium metal and chromium oxide surfaces. *Journal of Electron Spectroscopy and Related Phenomena*. 2011, vol. 184, pp. 29–37.

[9] SPEVACK, P.A., McINTYRE, N.S. Thermal reduction of MoO_3. *Journal of Physical Chemistry*. 1992, vol. 96, pp. 9029–9035.

[10] BIESINGER, M.C. *X-ray Photoelectron Spectroscopy (XPS) Reference Pages, Molybdenum* [online]. 2009–2021 [viewed: 2024-09-17]. Available from: http://www.xpsfitting.com/search/label/Molybdenum

[11] OKONKWO, I.A., DOFF, J., BARON-WIECHEC, A., JONES, G., KOROLEVA, E.V., SKELDON, P., THOMPSON, G.E. Oxidation states of molybdenum in oxide films formed in sulphuric acid and sodium hydroxide. *Thin Solid Films*. 2012, vol. 520, pp. 6318–6327.

[12] BIESINGER, M.C. *X-ray Photoelectron Spectroscopy (XPS) Reference Pages, Aluminum* [online]. 2009–2021 [viewed: 2024-09-16]. Available from: http://www.xpsfitting.com/search/label/Aluminum.

[13] STROHMEIER, B.R. An ESCA method for determining the oxide thickness on aluminum alloys. *Surface and Interface Analysis*. 1990, vol. 15, pp. 51–56.